Journal of Geophysical Research

The effects of pan-Arctic snow cover and air temperature changes on frozen soil heat content

Xiaogang Shi[1] and Dennis P. Lettenmaier[1]*

[1]*Department of Civil and Environmental Engineering,*

University of Washington, Seattle, Washington, USA

*Corresponding author:

Dennis P. Lettenmaier

University of Washington

Department of Civil and Environmental Engineering, Box 352700

Seattle, WA 98195-2700

dennisl@u.washington.edu

Phone: 206 543 2532

Fax: 206 616 6274

Abstract

As an indicator of changes in the land surface energy budget, soil heat content (SHC) arguably provides a more complete understanding of high latitude land surface warming than do soil temperatures, which are influenced by surface air temperature (SAT) as well as snow cover extent (SCE). Using the Variable Infiltration Capacity (VIC) land surface model forced with gridded climate observations, we are able to reproduce observed spatial and temporal variations of SCE and SHC over the pan-Arctic land region for the last half-century. On the basis of the SCE trends derived from NOAA satellite observations in 5° latitude bands from April through June for the period 1972-2006, we define a snow covered sensitivity zone (SCSZ), a snow covered non-sensitivity zone (SCNZ), and a non-snow covered zone (NSCZ) for North America and Eurasia. We then explore long-term trends in SHC, SCE, and SAT and their corresponding correlations in NSCZ, SCSZ and SCNZ for both North America and Eurasia. We find that snow cover recession has a significant impact on SHC changes in SCSZ for North America and Eurasia from April through June. SHC changes in SCSZ over North America are dominated by snow cover recession rather than increasing SAT. Over Eurasia, increasing SAT more strongly affects SHC than in North America. Overall, increasing SAT during late spring and early summer has the greatest influence on SHC changes over the pan-Arctic, and reduced SCE plays a secondary role, which is only significant in SCSZ.

1. Introduction

Over the pan-Arctic region (for purposes of this paper, defined as the land area draining to the Arctic Ocean), the rise in surface air temperature (SAT) has been almost twice as large as the global average in recent decades [Serreze et al., 2000; Jones and Moberg, 2003; Overland et al., 2004; Hinzman et al., 2005; White et al., 2007; Solomon et al., 2007; Trenberth et al., 2007; Screen and Simmonds, 2010]. Increases in SAT have been accompanied by increasing soil temperatures with deeper active layer thickness across permafrost regions and decreasing frozen soil depths in the seasonally frozen ground regions [Hinzman and Kane, 1992; Frauenfeld et al., 2004; Romanovsky et al., 2007]. Given the potential for releases of soil carbon to the atmosphere at warmer temperatures, warming of the land surface at high latitudes has attracted considerable scientific attention [Stieglitz et al., 2003; Heimann and Reichstein, 2008].

Observed soil temperatures across the pan-Arctic have been used as an indicator of climate change in past studies [Osterkamp and Romanovsky, 1999; Zhang et al., 2001; Smith et al., 2004; Beltrami et al., 2006; Romanovsky et al., 2002, 2007]. However, *in situ* soil temperatures are problematic because latent heat effects, which may be significant in regions with frozen soils [Troy, 2010], are neglected. Arguably, the heat content of the soil column is a better indicator of changes in the land surface energy budget because it provides an integrated measure that accounts for changes in temperature, moisture, and latent heat effects. For this reason, it has been used in various studies to document how the land surface responds to atmospheric changes [Levitus et al., 2001, 2005; Beltrami et al., 2002, 2006; Hansen et al., 2005; Troy, 2010]. For instance, using the Variable Infiltration Capacity (VIC) land surface

model [Liang et al., 1994; Cherkauer and Lettenmaier, 1999], Troy et al. [2012] showed that modeled soil temperature profiles and soil heat content (SHC) trends reproduced observed trends at high latitudes. Following these previous studies, we evaluate SHC trends and their causes, with particular attention to the pan-Arctic land region.

Because snow is a strong insulator, it limits the efficient communication of heat between the atmosphere and the ground, and thus plays an important role in determining how air temperature signals propagate into the soil column [Gold, 1963; Goodrich, 1982; Osterkamp and Romanovsky, 1996; Stieglitz et al., 2003; Zhang, 2005; Bartlett et al., 2005; Iwata et al., 2008; Lawrence and Slater, 2010]. In general, seasonal snow cover tends to result in relatively higher mean annual ground temperatures, especially at high latitudes where stable snow cover lasts from a few weeks to several months [Zhang, 2005].

In the visible satellite imagery produced by the National Oceanic and Atmospheric Administration (NOAA) [Robinson et al., 1993; Frei and Robinson, 1999], a substantial retreat of snow cover extent (SCE) has been observed during late spring and early summer in recent decades [Groisman et al., 1994; Déry and Brown, 2007; Brown et al., 2010; Shi et al., 2011, 2012]. Moreover, these negative SCE trends are well reproduced for both North America and Eurasia by simulations using the VIC model [Shi et al., 2012].

Recent studies have attempted to explain the impact of seasonal snow cover and air temperature on the ground thermal regime over the pan-Arctic by using soil temperature as an index [e.g., Zhang et al., 1997; Zhang and Stamnes, 1998; Romanovsky et al., 2002; Bartlett et al., 2004, 2005; Lawrence and Slater, 2010]. However, the interpretation of relationships

between seasonal snow cover and air temperature on the ground thermal regime is complicated because surface temperature is affected by multiple variables. An alternative approach is to use SHC as an indicator of changes in the ground thermal regime because it can provide a complete understanding of high latitude land surface warming.

In this paper, we explore the effects of snow cover recession and increases in SAT on SHC over the pan-Arctic, with particular emphasis on trends and variability during the late spring and early summer. In section 2, we describe the observations and model-derived data sets on which our analyses are based. In section 3, we explore trends in SHC and examine correlations between SCE, SAT, and SHC and the relative roles of snow cover recession and increasing SAT on SHC changes.

2. Data sets

2.1. Observed SCE and SAT data

Observed monthly values of SCE were extracted from the weekly snow cover and sea ice extent version 3.1 product for the Northern Hemisphere (http://nsidc.org/data/nsidc-0046.html), maintained at the National Snow and Ice Data Center (NSIDC). These data span the period October 1966 through June 2007 [Armstrong and Brodzik, 2007]. The data set is based on weekly maps of continental SCE produced by NOAA's National Environmental Satellite Data and Information Service (NESDIS) [Robinson et al., 1993; Frei and Robinson, 1999], which were derived from digitized versions of manual interpretations of Advanced Very High Resolution Radiometer (AVHRR), Geostationary Operational Environmental Satellite (GOES), and other visible band satellite data. We used a version of the data that has been

regridded to the NSIDC EASE grid with a spatial resolution of 25 km by Armstrong and Brodzik [2007]. Our study is restricted to the period from 1972 on since some charts between 1967 and 1971 are missing [Robinson, 2000]. Although ending the time series in 2006 leaves out some exceptionally low Arctic spring SCE values in recent years (e.g., 2008-2010), the non-parametric statistical method we used (section 3.2) is robust to modest changes in the length of the record analyzed. We did not include Greenland in the analyses since its snow cover is mainly perennial in nature. Brown et al. [2010] have compared this SCE record (commonly referred to as the NOAA weekly SCE record) with other available Arctic snow cover data sets. In general, their study and others [e.g., Wiesnet et al., 1987; Robinson et al., 1993] have found that the NOAA weekly SCE data are reliable for continental-scale studies of snow cover variability. They have become a widely used tool for deriving trends in climate-related studies [Groisman et al., 1994; Déry and Brown, 2007; Flanner et al., 2009; Derksen et al., 2010; Derksen and Brown, 2011; Shi et al., 2011, 2012], notwithstanding uncertainties in some parts of the domain for certain times of the year, such as summertime over northern Canada [Wang et al., 2005]. A more recent update to the data set we used (NOAA snow chart climate data record, CDR) is now available [Brown and Robinson, 2011], but the differences between the new CDR and the data set we used at the pan-Arctic scale are small [Shi et al., 2011].

Monthly SAT anomaly data were derived from the Climatic Research Unit [CRU, Brohan et al., 2006] (CRUTEM3 data set from http://www.cru.uea.ac.uk/cru/data/temperature/), which are based on anomalies from the long-term mean temperature for the period 1961-1990

and are available for each month since 1850. The land-based monthly data are on a regular 0.5° by 0.5° global grid. We regridded these data, including the NOAA SCE observations that were aggregated from the 25-km product, to the 100-km EASE grid using an inverse distance interpolation as implemented in Shi et al. [2012].

2.2. Modeled SHC

The version of VIC used for this study is 4.1.2, which includes some updates to the model's algorithms for cold land processes. For instance, the model includes a snow parameterization that represents snow accumulation and ablation processes using a two-layer energy and mass balance approach [Andreadis et al., 2009], a canopy snow interception algorithm when an overstory is present [Storck et al., 2002], a finite-difference frozen soils algorithm [Cherkauer and Lettenmaier, 1999] with sub-grid frost variability [Cherkauer and Lettenmaier, 2003], and an algorithm for the sublimation and redistribution of blowing snow [Bowling et al., 2004], as well as a lakes and wetlands model [Bowling and Lettenmaier, 2010]. In our implementation of the VIC model, each grid cell is partitioned into five elevation (snow) bands, which can include multiple land cover types (tiles). The snow model is then applied to each tile separately. The current version of the frozen soils algorithm uses a finite difference solution in the algorithm that dates to the work of Cherkauer and Lettenmaier [1999]. To improve spring peak flow predictions, a parameterization of the spatial distribution of soil frost was developed [Cherkauer and Lettenmaier, 2003]. Adam [2007] described some significant modifications to the frozen soils algorithm, including the bottom boundary specification using the observed soil temperature datasets of Zhang et al. [2001], the exponential thermal node distribution, the implicit solver using the Newton-Raphson method, and an excess ground ice

and ground subsidence algorithm in VIC 4.1.2. In order to model permafrost properly, our implementation used a depth of 15 m with 18 thermal nodes exponentially distributed with depth and a no flux bottom boundary condition [Jennifer Adam, personal communication], which is similar to Troy et al. [2012].

We used the same study domain as documented in Shi et al. [2012], which is defined as all land areas draining into the Arctic Ocean, as well as those regions draining into the Hudson Bay, Hudson Strait, and the Bering Strait, but excluding Greenland (because its snow cover is mainly perennial in nature). The model simulations used calibrated parameters, such as soil depths and infiltration characteristics, from Su et al. [2005]. The off-line VIC runs are at a three-hour time step in full energy balance mode (meaning that the model closes a full surface energy budget by iterating for the effective surface temperature, as contrasted with water balance mode, in which the surface temperature is assumed to equal the surface air temperature) forced with daily precipitation, maximum and minimum temperatures, and wind speed at a spatial resolution (EASE grid) of 100 km. The forcing data were constructed from 1948 through 2006 using methods outlined by Adam and Lettenmaier [2008], as described in Shi et al. [2012]. To set the initial conditions including the thermal state in VIC, we initialized the model with a 100-year climatology created by randomly sampling years from the 1948-1969 meteorological forcings. Using VIC 4.1.2, we reconstructed SHC from 1970 to 2006 for the pan-Arctic land area.

3. Results

3.1. Definition of study zones

173 The NOAA weekly SCE data (hereafter NOAA-SCE) were analyzed to determine
174 whether or not there are regions with significant changes of NOAA-SCE in North America and
175 Eurasia. On the basis of the SCE trends derived from NOAA-SCE in 5° latitude bands from
176 April through June for the period 1972-2006 as described in Shi et al. [2012], we defined a
177 snow covered sensitivity zone (SCSZ), a snow covered non-sensitivity zone (SCNZ), and a
178 non-snow covered zone (NSCZ) for North America and Eurasia, respectively.

179 Figure 1(a) shows the spatial distribution of long-term monthly means of SCE from
180 NOAA-SCE from April through June for the 35-year period over North American and
181 Eurasian pan-Arctic domains. Figures 1 (b) and (c) illustrate the latitudinal variations of SCE
182 trends and their area fractions over the North American and Eurasian study domains from April
183 through June. The percentage under each bar chart is the trend significance expressed as a
184 confidence level for each 5° of latitude, while the solid line shows the latitudinal patterns in the
185 snow cover area fractions for each month, which in general are at a minimum for the lowest
186 latitude band, and then increase with latitude poleward.

187 Based on the latitudinal changes of NOAA-SCE as shown in Figure 1, we identified
188 different study zones for North America and Eurasia. From April through June, snow mostly
189 covers latitude bands north of 45°N over the pan-Arctic land area, which are denoted as snow
190 covered zones (SCZs) in Figure 1. The rest of the study domains were denoted as non-snow
191 covered zones (NSCZs) (see Figure 1(a) for North America and Eurasia, respectively). Within
192 the SCZs, we selected only those latitudinal bands within which SCE trends were statistically
193 significant for further analyses. For each month, we denoted these bands as snow cover
194 sensitivity zones (SCSZs). For the remaing bands in the SCZs, there is no significant snow

cover recession, and these bands are defined as snow covered non-sensitivity zones (SCNZs). In Figures 1(b) and 1(c), we use different gray-shaded arrows to highlight the North American and Eurasian SCZs, which include the SCSZs and SCNZs. For example, the SCSZ for May in North America has six latitude bands from 45-50°N to 70-75°N, whereas there is only one band (45-50°N) for the Eurasian SCSZ in April.

3.2. Experimental design based on SCE and SAT trends

Trend tests were performed on the monthly time series of SCE and SAT area-averaged over the North America and Eurasia study zones. We used the non-parametric Mann-Kendall trend test [Mann, 1945] for trend significance, and the Sen method [Sen, 1968] to estimate their slopes. A 5% significance level (two-tailed test) was used. Tables 1 and 2 summarize the SCE and SAT trends and their significance levels in NSCZ, SCSZ, and SCNZ for both continents from April through June for the entire study period (1972-2006). Table 1 shows that strong statistically significant ($p < 0.025$) negative trends were detected in SCE for both North American and Eurasian SCSZs, as found in many previous studies. In SCNZ, the decreasing trends in SCE are all non-significant, and the absolute values of trend slopes are much smaller than that in SCSZ. As reported in Table 2, increasing SAT trends were detected for both continents except for North America in May. For June in North America and for May and June in Eurasia, these SAT trends are statistically significant in NSCZ, SCSZ, and SCNZ. In SCNZ, increasing SAT trends are all statistically significant for both continents except for Eurasia in April.

215 Based on above long-term trends in SCE and SAT for NSCZ, SCSZ, and SCNZ, it is
216 clear that the impact of increasing SAT on SHC changes can be isolated in NSCZ as there is no
217 presence of snow. In SCSZ, the effects of both SCE and SAT changes on SHC can be
218 compared as indicated in Figure 2. By comparing SCSZ and SCNZ, we can investigate the
219 effect of snow cover recession on SHC changes, as there is snow cover recession in SCSZ
220 whereas none is in SCNZ. Figure 3 shows the area percentages for NSCZ, SCSZ and SCNZ in
221 North America and Eurasia from April through June. In Eurasia, the SCNZ dominates in April
222 as there is no significant snow cover recession for most portions of the study domain. When
223 snow cover retreats, the SCSZ and NSCZ in Eurasia expands significantly in May and June.
224 Over North America, the NOAA-SCE recession occurs earlier than in Eurasia. Especially for
225 May, most regions in North America have snow cover recession. In June, Figure 3 clearly
226 illusrates that SCE is already gone for most portions of Eurasia.

227 **3.3. SHC trends**

228 Recent studies by Troy et al. [2012] have shown that the VIC model is able to
229 reproduce soil temperature profiles and can be used as a surrogate for (scarce) observations to
230 estimate long-term changes in SHC. To maximize computational efficiency, the spacing of soil
231 thermal nodes in the frozen soils framework in VIC should reflect the variability in soil
232 temperature [Adam, 2007]. Because the greatest variability in soil temperature occurs near the
233 surface, it is preferable to have tighter node spacings near the surface and wider node spacings
234 near the bottom boundary where temperature variability is reduced. Therefore, we used
235 eighteen soil thermal nodes (STNs) distributed exponentially with depth as indicated in Table 3.

236 The SHC for each STN in the soil column was calculated for each model time step
237 (three hours) and then aggregated for each month from April through June. Along the soil
238 profile from the top to the bottom, the first STN was named as STN0 with a depth of 0m
239 indicating it is at the surface, while the deepest one is STN17 with a depth of 15m. The SHC
240 for STN17 represents an averaged thermal value for the soil profile. To simplify the analyses,
241 we used the mean monthly SHC in 1970 as zero because the change in soil heat is relative to
242 the datum chosen as described in Troy [2010]. All monthly SHC values are relative to this
243 datum. In addition, monthly SHC anomalies were calculated on the basis of monthly means
244 averaged over each NSCZ, SCSZ and SCNZ of North America and Eurasia by removing the
245 1981-1990 mean. To examine long-term trends in the time series of monthly SHC anomalies,
246 the Mann-Kendall trend test (significance level $p < 0.025$, two-sided test) and the Sen method
247 as described above were applied. For each study zone, monotonic trend tests were performed
248 on the monthly SHC anomalies averaged over each study zone for each soil thermal node.

249 Figure 4 shows the trends and significance levels of the VIC-derived SHC for each
250 STN in NSCZ, SCSZ and SCNZ over North America and Eurasia from April through June.
251 Figures 4a and 4b show that there are obvious differences for trends and significance levels
252 between North America and Eurasia. For North America (Figure 4a), the SHC in SCSZ
253 increases significantly from the top thermal nodes to the deeper ones, whereas in NSCZ and
254 SCNZ, most thermal nodes have increasing trends, which are not statistically significant. Over
255 Eurasia, this is quite different. In Figure 4b, almost all the thermal nodes in NSCZ, SCSZ, and
256 SCNZ over Eurasia from April through June show statistically significant increasing trends in

SHC, indicating that there are different effects of snow cover recession and increasing SAT on SHC changes between Eurasia and North America.

3.4. Effects of SCE and SAT changes on SHC

In order to identify the relative roles of snow cover recession and increasing SAT on pan-Arctic SHC changes, we examined the correlations among SHC, SCE, and SAT over NSCZ, SCSZ and SCNZ for both North America and Eurasia. The Pearson's product-moment correlation coefficient was computed separately for each study zone from April through June. Given the 35-year record, correlations are statistically significant at a level of $p < 0.025$ (two-sided) when the absolute value of the sample correlation is greater than 0.34 based on the Student t-test with 33 degrees of freedom. Figure 5 shows correlations between observed SCE and VIC-derived SHC in NSCZ, SCSZ, and SCNZ over North America and Eurasia from April through June. In SCSZ, the correlations between SHC and SCE are all statistically significant over both continents from April through June. Over SCNZ, however, the correlations are much smaller and have no statistical significance. These results imply that the static snow cover insulation in SCNZ has a non-significant impact on SHC changes over the pan-Arctic. Additionally, no correlation exists between SHC and SCE in NSCZ. Furthermore, the implied impact of snow cover changes on SHC is similar for North America and Eurasia.

Figure 6 shows correlations between observed SAT and simulated SHC monthly time series in NSCZ, SCSZ, and SCNZ over North America and Eurasia from April through June. Overall, the results indicate that SAT has a significant impact on SHC changes in NSCZ.

277 Moreover, SAT has greater influence on SHC over Eurasia than in North America as shown in
278 Figure 6. All the correlations over Eurasia are statistically significant except for SCSZ and
279 SCNZ in April, for which the increasing trends in SAT are not statistically significant.

280 The correlations described in Figures 5 and 6 were calculated on the time series of
281 variables using the Pearson's product-moment method. Both the effects of secular trend and
282 variability are included. We separated these two components and explored the relative roles of
283 the linear trend and the variability (detrended) in the corresponding correlations. Table 4
284 summarizes correlation coefficients due to the linear trend and the variability between SHC
285 derived from VIC and NOAA-SCE observations in SCSZ and SCNZ over North America and
286 Eurasia for the period 1972-2006. The significance level (*p*-value) was calculated using a two-
287 tailed Student t-test with 33 degrees of freedom. Basically, SHC and NOAA-SCE in NSCZ,
288 SCSZ, and SCNZ are highly correlated due to the secular trend, except for May and June in
289 SCNZ over North America, where the NOAA-SCE trends are zero. In contrast, the variability
290 components are small without statistical significance. Obviously, the relationships between
291 SHC and NOAA-SCE time series are mainly dominated by snow cover changes in each study
292 zone over North America and Eurasia. We also applied the same analyses for the VIC-derived
293 SHC and CRU SAT, as reported in Table 5. The linear trends in SAT dominate the correlations
294 between SHC derived from VIC and CRU SAT in NSCZ, SCSZ, and SCNZ over North
295 America and Eurasia for the period 1972-2006. In contrast, the effect of SAT variability is
296 weak and not statistically significant. Therefore, the relationships between SHC and SAT time
297 series as shown in Figure 6 are mainly due to increasing SAT in each study zone over North
298 America and Eurasia.

As described above, SHC changes are significantly affected by snow cover recession and increasing SAT from April through June over North America and Eurasia for the period 1972-2006. But the variablity in NOAA-SCE and SAT has a insignificant effect on SHC. Comparing the correlations in Figures 5 and 6 suggests that: (1) snow cover recession has a significant impact on SHC changes in SCSZ, which is similar for both continents; (2) SHC changes in SCSZ over North America during late spring and early summer are dominated by snow cover recession rather than increasing SAT; (3) over Eurasia, increasing SAT more strongly affects SHC than in North America; and (4) overall, increasing SAT has the greatest influence on SHC for North America and Eurasia, and reduced SCE plays a secondary role, which is only significant in SCSZ.

4. Conclusions

We defined three study zones (NSCZ, SCSZ, and SCNZ) within the North American and Eurasian portions of the pan-Arctic land area based on observed SCE trends. Using these definitions of zones, we focused on the effects of pan-Arctic snow cover and air temperature changes on SHC by exploring long-term trends in SHC, SCE, and SAT and their corresponding correlations in NSCZ, SCSZ, and SCNZ for North America and Eurasia. We find that North American and Eurasian late spring and early summer (from April through June) SHC has increasing trends for the period 1972-2006. However, there are obvious differences between North America and Eurasia as to the magnitudes of SHC trend slopes and significance levels. For North America, SHC in SCSZ has mostly increased significantly, whereas in NSCZ and SCNZ, most thermal nodes show non-significant increasing trends. For Eurasia, almost all the thermal nodes in NSCZ, SCSZ, and SCNZ have statistically significant increasing trends,

indicating that there are different effects of snow cover recession and increasing SAT on SHC changes between North America and Eurasia. By analyzing the corresponding correlations, we conclude that snow cover recession has a significant impact on SHC changes in SCSZ for North America and Eurasia from April through June. SHC changes in SCSZ over North America are dominated by snow cover recession rather than increasing SAT. Over Eurasia, increasing SAT more strongly affects SHC than in North America. Overall, increasing SAT during late spring and early summer has the greatest influence on SHC changes over the pan-Arctic, and reduced SCE plays a secondary role, which is only significant in SCSZ.

329 **Acknowledgements**

330 This work was supported by NASA grants NNX07AR18G and NNX08AU68G to the
331 University of Washington. The authors thank Dr. Tara Troy from Columbia University, Dr.
332 Jennifer Adam from Washington State University, and Mr. Ted Bohn and Miss Elizabeth Clark
333 from the University of Washington for their assistance and comments.

334

335 **References**

336 Adam, J. C. (2007), Understanding the causes of streamflow changes in the Eurasian Arctic,
337 Ph.D. thesis, 174pp., University of Washington, Seattle, WA.

338 ——, and D. P. Lettenmaier (2008), Application of new precipitation and reconstructed
339 streamflow products to streamflow trend attribution in northern Eurasia. *J. Clim., 21,*
340 1807-1828.

341 Andreadis, K. M., P. Storck, and D. P. Lettenmaier (2009), Modeling snow accumulation and
342 ablation processes in forested environments, *Water Resour. Res., 45,* W05429,
343 doi:10.1029/2008WR007042.

344 Armstrong, R. L., and M. J. Brodzik (2007), Northern Hemisphere EASE-Grid weekly snow
345 cover and sea ice extent version 3.1, National Snow and Ice Data Center, Boulder, CO,
346 digital media. [Available online at http://nsidc.org/data/nsidc-0046.html.]

347 Bartlett, M. G., D. S. Chapman, and R. N. Harris (2004), Snow and the ground temperature
348 record of climate change, *J. Geophys. Res., 109*, F04008, doi:10.1029/2004JF000224.

349 Bartlett, M. G., D. S. Chapman, and R. N. Harris (2005), Snow effect on North American
350 ground temperatures, 1950-2002, *J. Geophys. Res., 110,* F03008,
351 doi:10.1029/2005JF000293.

352 Beltrami, H., J. Smerdon, H. N. Pollack, and S. Huang (2002), Continental heat gain in the
353 global climate system, *Geophys. Res. Lett., 29(8),* 1167, doi:10.1029/2001GL014310.

354 Beltrami, H., E. Bourlon, L. Kellman, and J. F. Gonza´lez-Rouco (2006), Spatial patterns of

355 ground heat gain in the Northern Hemisphere, *Geophys. Res. Lett., 33,* L06717,
356 doi:10.1029/2006GL025676.

357 Bowling, L. C., J. W. Pomeroy, and D. P. Lettenmaier (2004), Parameterization of blowing-
358 snow sublimation in a macroscale hydrology model, *J. Hydrometeorol., 5,* 745-762.

359 Bowling, L. C., and D. P. Lettenmaier (2010), Modeling the effects of lakes and wetlands on
360 the water balance of arctic environments, *J. Hydrometeorol., 11(2),* 276-295.

361 Brohan, P., J. Kennedy, I. Harris, S. Tett, and P. Jones (2006), Uncertainty estimates in
362 regional and global observed temperature changes: A new dataset from 1850, *J.*
363 *Geophys. Res., 111,* D12106.

364 Brown, R. D., C. Derksen, and L. Wang (2010), A multi-data set analysis of variability and
365 change in Arctic spring snow cover extent, 1967-2008, *J. Geophys. Res., 115,* D16111.

366 Brown, R. D., and D. A. Robinson (2011), Northern Hemisphere spring snow cover variability
367 and change over 1922–2010 including an assessment of uncertainty, *The Cryosphere, 5,*
368 219-229.

369 Cherkauer, K. A. and D. P. Lettenmaier (1999) Hydrologic effects of frozen soils in the upper
370 Mississippi River basin, *J. Geophys. Res., 104,* 19599-19610.

371 —— (2003), Simulation of spatial variability in snow and frozen soil, *J. Geophys. Res., 108,*
372 8858.

373 Déry, S. J., and R. D. Brown (2007), Recent Northern Hemisphere snow cover extent trends
374 and implications for the snow-albedo feedback, *Geophys. Res. Lett., 34,* L22504, doi:

10.1029/2007GL031474.

Derksen, C., and R. D. Brown (2011), Terrestrial snow (Arctic) in state of the climate in 2010, *Bull. Am. Meteorol. Soc., 92,* S154-S155.

——, and L. Wang (2010), Terrestrial snow (Arctic) in state of the climate in 2009, *Bull. Am. Meteorol. Soc., 91,* S93-S94.

Flanner, M., C. Zender, P. Hess, N. Mahowald, T. Painter, V. Ramanathan, and P. Rasch (2009), Springtime warming and reduced snow cover from carbonaceous particles, *Atmos. Chem. Phys., 9,* 2481-2497.

Frauenfeld, O. W., T. Zhang, R. G. Barry, and D. Gilichinsky (2004), Interdecadal changes in seasonal freeze and thaw depths in Russia, *J. Geophys. Res., 109,* D05101, doi:10.1029/2003JD004245

Frei, A., and D. A. Robinson (1999), Northern Hemisphere snow extent: Regional variability 1972-1994, *Int. J. Climatol., 19,* 1535-1560.

Gold, L. W. (1963), Influence of snow cover on the average annual ground temperature at Ottawa, Canada, *IAHS Publ., 61,* 82-91.

Goodrich, L. E. (1982), The influence of snow cover on the ground thermal regime, *Canadian Geotechnical J., 24,* 160-163.

Groisman, P. Y., T. R. Karl, R. W. Knight, and G. L. Stenchikov (1994), Changes of snow cover, temperature, and radiative heat balance over the Northern Hemisphere, *J. Clim., 7,* 1633-1656.

Hansen, J., et al. (2005), Earth's energy imbalance: Confirmation and implications, *Science,*

308, 1431-1435.

Heimann, M., and M. Reichstein (2008), Terrestrial ecosystem carbon dynamics and climate feedbacks, *Nature, 451*(7176), 289-292.

Hinzman, L. D., and D. L. Kane (1992), Potential response of an Arctic watershed during a period of global warming, *J. Geophys. Res., 97,* 2811-2820.

Hinzman, L. D., and Coauthors (2005), Evidence and implications of recent climate change in northern Alaska and other arctic regions, *Clim. Change, 72,* 251-298.

Iwata, Y., M. Hayashi, and T. Hirota (2008), Effects of snow cover on soil heat flux and freeze-thaw processes, *J. Agric. Meteorol., 64,* 301-308.

Jones, P. D., and A. Moberg (2003), Hemispheric and large-scale surface air temperature variations: An extensive revision and an update to 2001, *J. Clim., 16,* 206-223.

Lawrence, D. M., and A. G. Slater (2010), The contribution of snow condition trends to future ground climate, *Clim. Dyn., 34,* 969-981, doi:10.1007/s00382-009-0537-4.

Levitus, S., J. Antonov, J. Wang, T. L. Delworth, K. Dixon, and A. Broccoli (2001), Anthropogenic warming of the Earth's climate system, *Science, 292,* 267-270.

Levitus, S., J. Antonov, and T. Boyer (2005), Warming of the world ocean, 1955-2003, *Geophys. Res. Lett., 32,* L02604, doi:10.1029/2004GL021592.

Liang, X., D. P. Lettenmaier, E. Wood, and S. Burges (1994), A simple hydrologically based model of land surface water and energy fluxes for general circulation models, *J. Geophys. Res., 99,* D17, 14415-14428.

Mann, H. B. (1945), Nonparametric tests against trend, *J. Econom. Sci.*, 245-259.

Osterkamp, T. E., and V. E. Romanovsky (1996), Characteristics of changing permafrost temperatures in the Alaskan Arctic, U.S.A., *Arct. Alp. Res., 28(3),* 167-273.

Osterkamp, T. E., and V. E. Romanovsky (1999), Evidence for warming and thawing of discontinuous permafrost in Alaska, *Permafr. Periglac. Process., 10(1),* 17-37.

Overland, J. E., M. C. Spillane, D. B. Percival, M. Y. Wang, and H. O. Mofjeld (2004), Seasonal and regional variation of pan-Arctic surface air temperature over the instrumental record, *J. Clim., 17*, 3263-3282.

Robinson, D. A. (2000), Weekly Northern Hemisphere snow maps: 1966-1999, Preprints, *12th Conf. on Applied Climatology*, Asheville, NC, Amer. Meteor. Soc., 12-15.

——, K. F. Dewey, and R. R. Heim Jr (1993), Global snow cover monitoring: An update, *Bull. Amer. Meteor. Soc., 74,* 1689-1696.

Romanovsky, V., S. Smith, K. Yoshikawa, and J. Brown (2002), Permafrost temperature records: indicators of climate change, *EOS, Transactions of AGU, 83,* 589-594.

Romanovsky, V. E., T. S. Sazonova, V. T. Balobaev, N. I. Shender, and D. O. Sergueev (2007), Past and recent changes in air and permafrost temperatures in eastern Siberia, *Global Planet. Change, 56*, 399-413.

Screen, J. A., and I. Simmonds (2010), The central role of diminishing sea ice in recent Arctic temperature amplification, *Nature, 464*,1334-1337.

Sen, P. K. (1968), Estimates of the regression coefficient based on Kendall's tau, *J. Am. Stat.*

436 *Assoc.*, 1379-1389.

437 Serreze, M., and Coauthors (2000), Observational evidence of recent change in the northern
438 high-latitude environment, *Clim. Change, 46,* 159-207.

439 Shi, X., P. Y. Groisman, S. J. Déry, and D. P. Lettenmaier (2011), The role of surface energy
440 fluxes in pan-Arctic snow cover changes, *Environ. Res. Lett., 6,* 035204.

441 Shi, X., S. J. Déry, P. Y. Groisman, and D. P. Lettenmaier (2012), Relationships between
442 recent pan-Arctic snow cover and hydroclimate trends, *J. Clim.* (in press).

443 Smith, N. V., S. S. Saatchi, and J. T. Randerson (2004), Trends in high northern latitude soil
444 freeze and thaw cycle from 1988 to 2002, *J. Geophys. Res., 109,* D12101,
445 doi:10.1029/2003JD004472

446 Solomon, S., D. Qin, M. Manning, M. Marquis, K. Averyt, M. M. B. Tignor, H. L. Miller Jr.,
447 and Z. Chen, Eds. (2007), *Clim. Change 2007: The Physical Science Basis,* Cambridge
448 University Press, 996 pp.

449 Stieglitz, M., S. J. Déry, V. E. Romanovsky, and T. E. Osterkamp (2003), The role of snow
450 cover in the warming of arctic permafrost, *Geophys. Res. Lett., 30,* 1721, doi:
451 10.1029/2003GL017337.

452 Storck, P., D. P. Lettenmaier, and S. M. Bolton (2002), Measurement of snow interception and
453 canopy effects on snow accumulation and melt in a mountainous maritime climate,
454 Oregon, United States, *Water Resour. Res., 38,* 1223.

455 Su, F., J. C. Adam, L. C. Bowling, and D. P. Lettenmaier (2005), Streamflow simulations of

456 the terrestrial Arctic domain, *J. Geophys. Res., 110*, 0148-0227.

457 Trenberth, K. E., et al. (2007), Observations: Surface and atmospheric climate change, in
458 *Climate Change 2007: The Physical Science Basis, contribution of working group I to*
459 *the fourth assessment report of the intergovernmental panel on climate change*, edited
460 by S. Solomon et al., 235-336, Cambridge Univ. Press, New York.

461 Troy, T. J. (2010), The hydrology of northern Eurasia: uncertainty and change in the terrestrial
462 water and energy budgets, Ph.D. thesis, 164pp., Princeton University, Princeton, NJ.

463 ——, J. Sheffield, and E. F. Wood (2012), Accelerating soil heat accumulation across northern
464 Eurasia, *J. Clim.* (submitted).

465 Wang, L., M. Sharp, R. Brown, C. Derksen, and B. Rivard (2005), Evaluation of spring snow
466 covered area depletion in the Canadian Arctic from NOAA snow charts, *Remote Sens.*
467 *Environ., 95*, 453-463.

468 White, D., and Coauthors (2007), The arctic freshwater system: changes and impacts, *J.*
469 *Geophys. Res., 112*, G04S54, doi:10.1029/2006JG000353.

470 Wiesnet, D., C. Ropelewski, G. Kukla, and D. Robinson (1987), A discussion of the accuracy
471 of NOAA satellite-derived global seasonal snow cover measurements, Proc. Vancouver
472 Symp.: Large Scale Effects of Seasonal Snow Cover, Vancouver, BC, Canada, *IAHS*
473 *Publ. 166*, 291-304.

474 Zhang, T., T. E. Osterkamp, and K. Stamnes (1997), Effects of climate on the active layer and
475 permafrost on the North Slope of Alaska, U.S.A., *Permafr. Periglac. Process., 8*, 45-67.

476 Zhang, T., and K. Stamnes (1998), Impact of climatic factors on the active layer and
477 permafrost at Barrow, Alaska, *Permafr. Periglac. Process., 9,* 229-246.

478 Zhang, T., R. G. Barry, D. Gilichinsky, S. S. Bykhovets, V. A. Sorokovikov, and J. P. Ye
479 (2001), An amplified signal of climatic change in soil temperatures during the last
480 century at Irkutsk, Russia, *Clim. Change, 49*, 41-76.

481 Zhang, T. (2005), Influence of the seasonal snow cover on the ground thermal regime: An
482 overview, *Rev. Geophys., 43,* RG4002, doi:10.1029/2004RG000157.

List of Figures

500 **Figure 6.** Correlations between observed SAT and simulated SHC in NSCZ, SCSZ and SCNZ
501 over North America and Eurasia from April through June for the period 1972-2006. The
502 correlation is statistically significant at a level of $p < 0.025$ when its absolute value is greater
503 than 0.34.

504

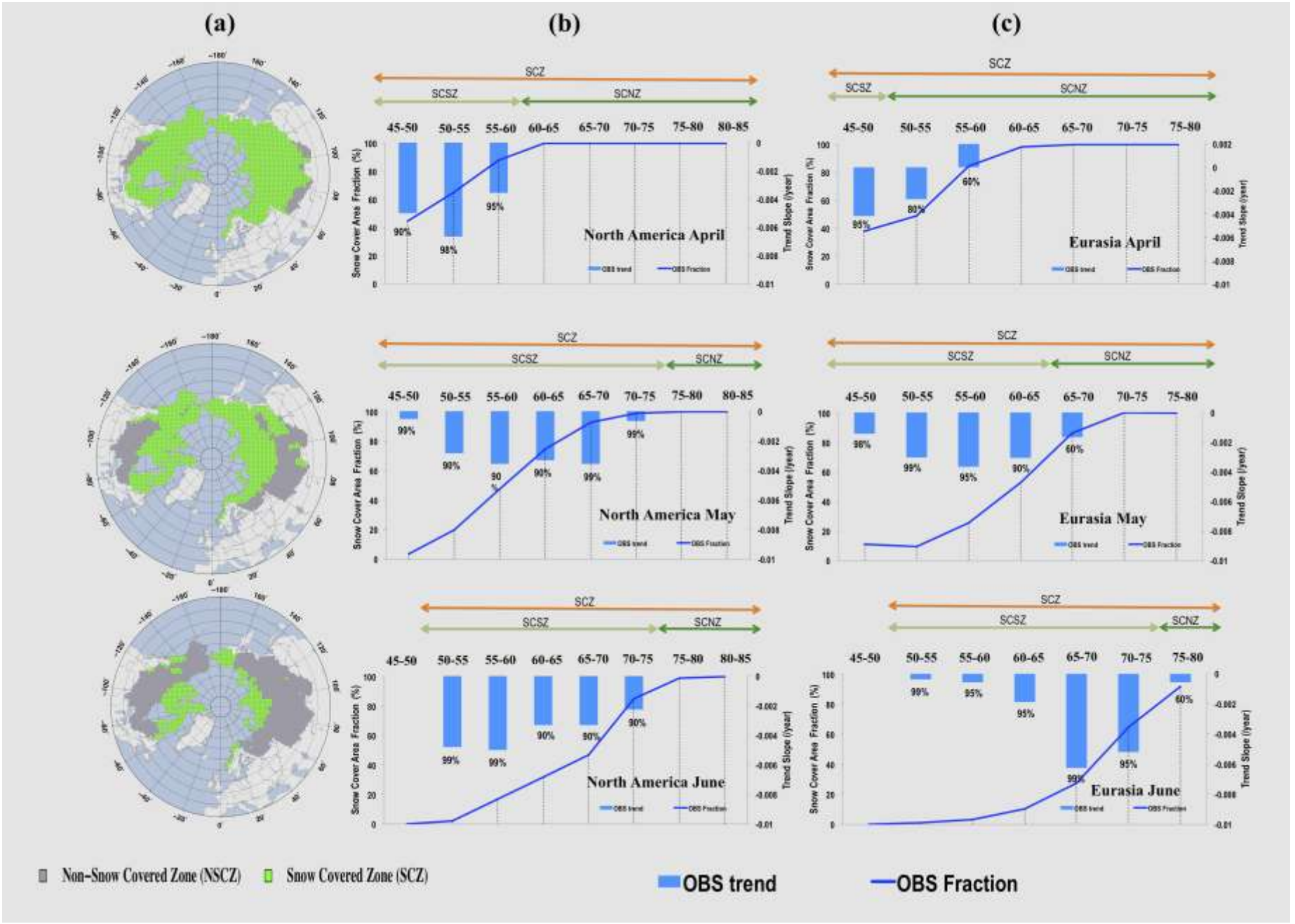
(a)
(b)
(c)
SCZ
SCSZ
SCNZ
45-50
50-55
55-60
60-65
65-70
70-75
75-80
80-85
Snow Cover Area Fraction (%)
Trend Slope (/year)
North America April
Eurasia April
North America May
Eurasia May
North America June
Eurasia June
OBS trend
OBS Fraction
Non-Snow Covered Zone (NSCZ)
Snow Covered Zone (SCZ)

505

Figure 1. (a) Spatial distribution of monthly mean snow cover extent (SCE) from NOAA satellite observations (OBS) over North America and Eurasia in the pan-Arctic land region (non-snow covered zone (NSCZ) and snow covered zone (SCZ)) for April (top panel), May (middle panel), and June (bottom panel) for the period 1972-2006. The SCE trends in 5° latitude bands and their area fractions over (b) North American and (c) Eurasian SCZ, including the snow covered sensitivity zone (SCSZ) and snow covered non-sensitivity zones (SCNZ) as indicated by the arrows. The percentage under each bar chart is the trend significance for each 5° (N) of latitude (expressed as a confidence level (CL)).

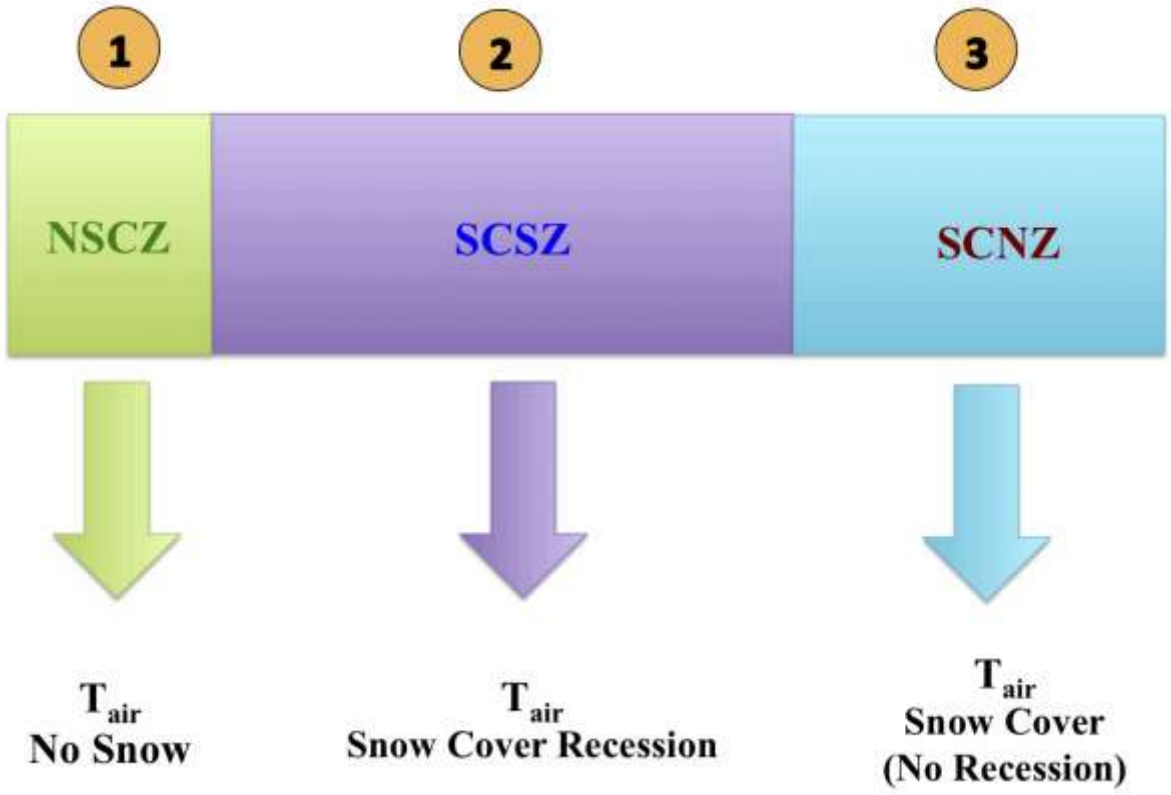

Figure 2. Experimental design for accessing the effects of pan-Arctic snow cover and air temperature changes on frozen soil heat content (SHC) in NSCZ, SCSZ, and SCNZ over North America and Eurasia from April through June for the period 1972-2006.

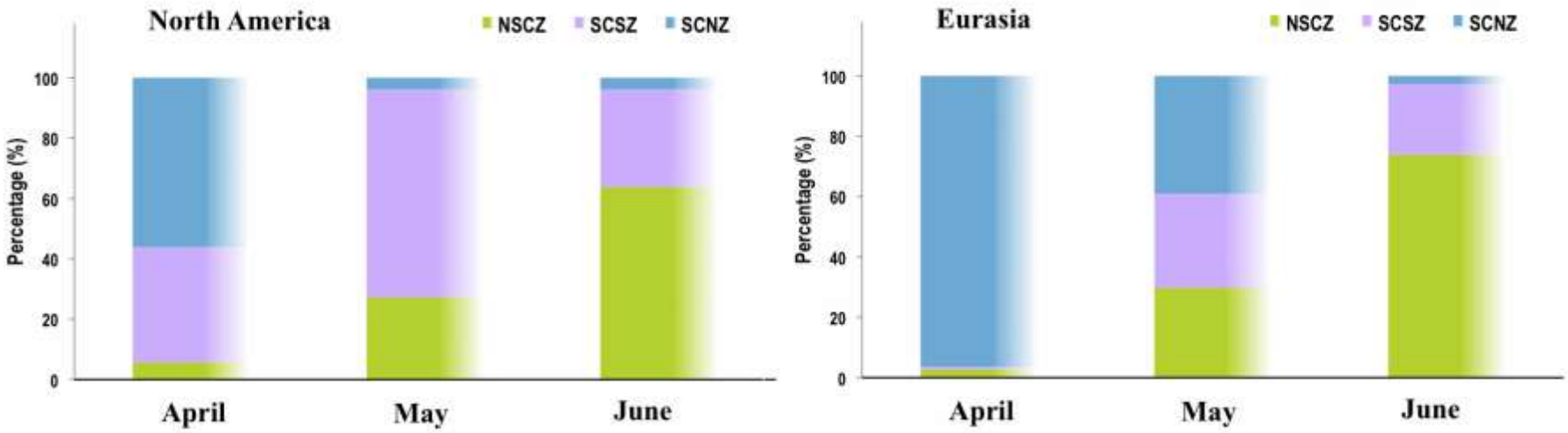

Figure 3. Area comparisons of NSCZ, SCSZ, and SCNZ in North America and Eurasia from April through June for the period 1972-2006.

529

530

(a)

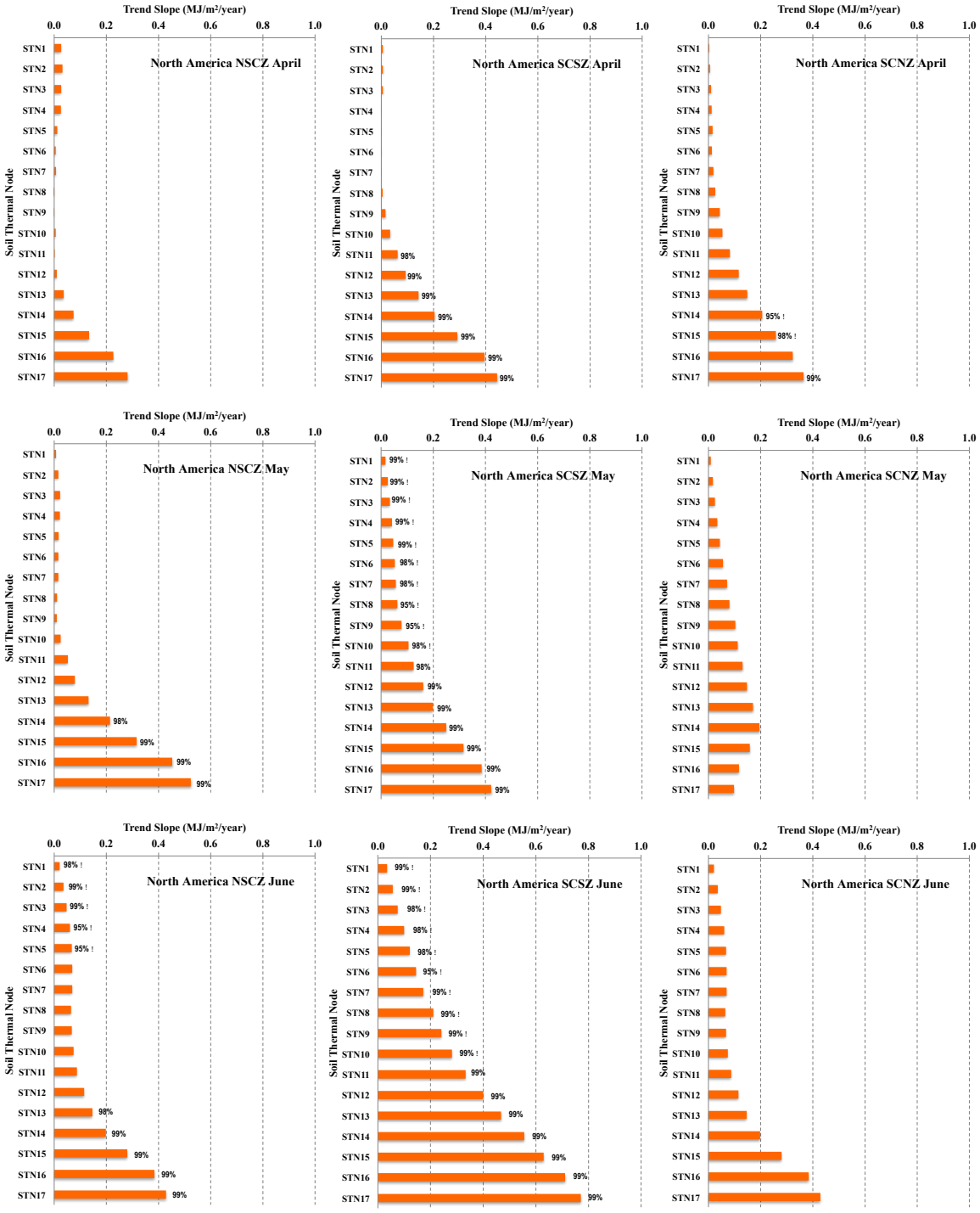

531

532

533

(b)

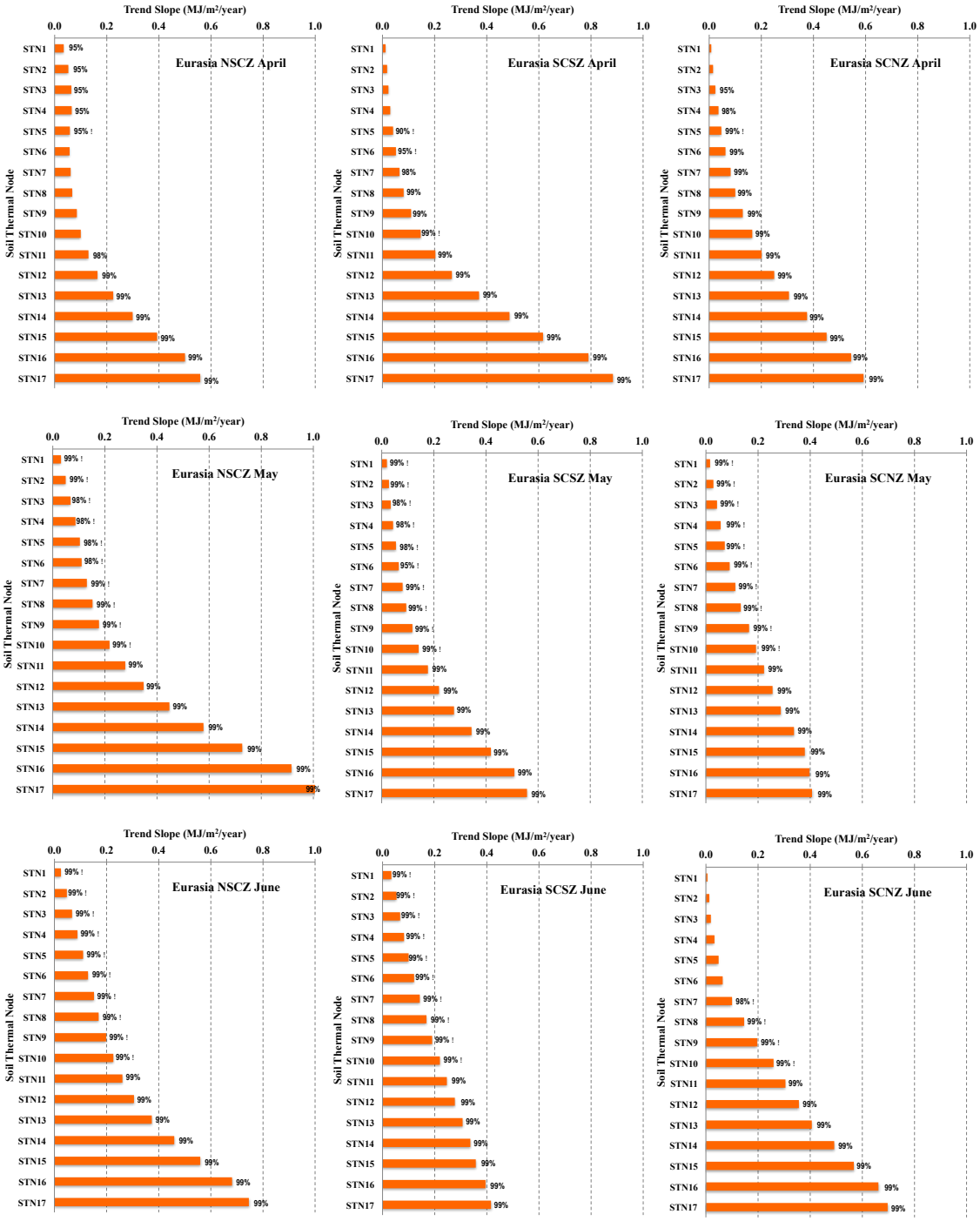

Figure 4. Trend analyses for SHC at the depth of each soil thermal node derived from the VIC model in NSCZ, SCSZ, and SCNZ over (a) North America and (b) Eurasia from April through June for the period 1972-2006. The significance level (expressed as a CL) was calculated using a two-sided Mann-Kendall trend test. Trend slope (TS) units are $mJm^{-2}year^{-1}$.

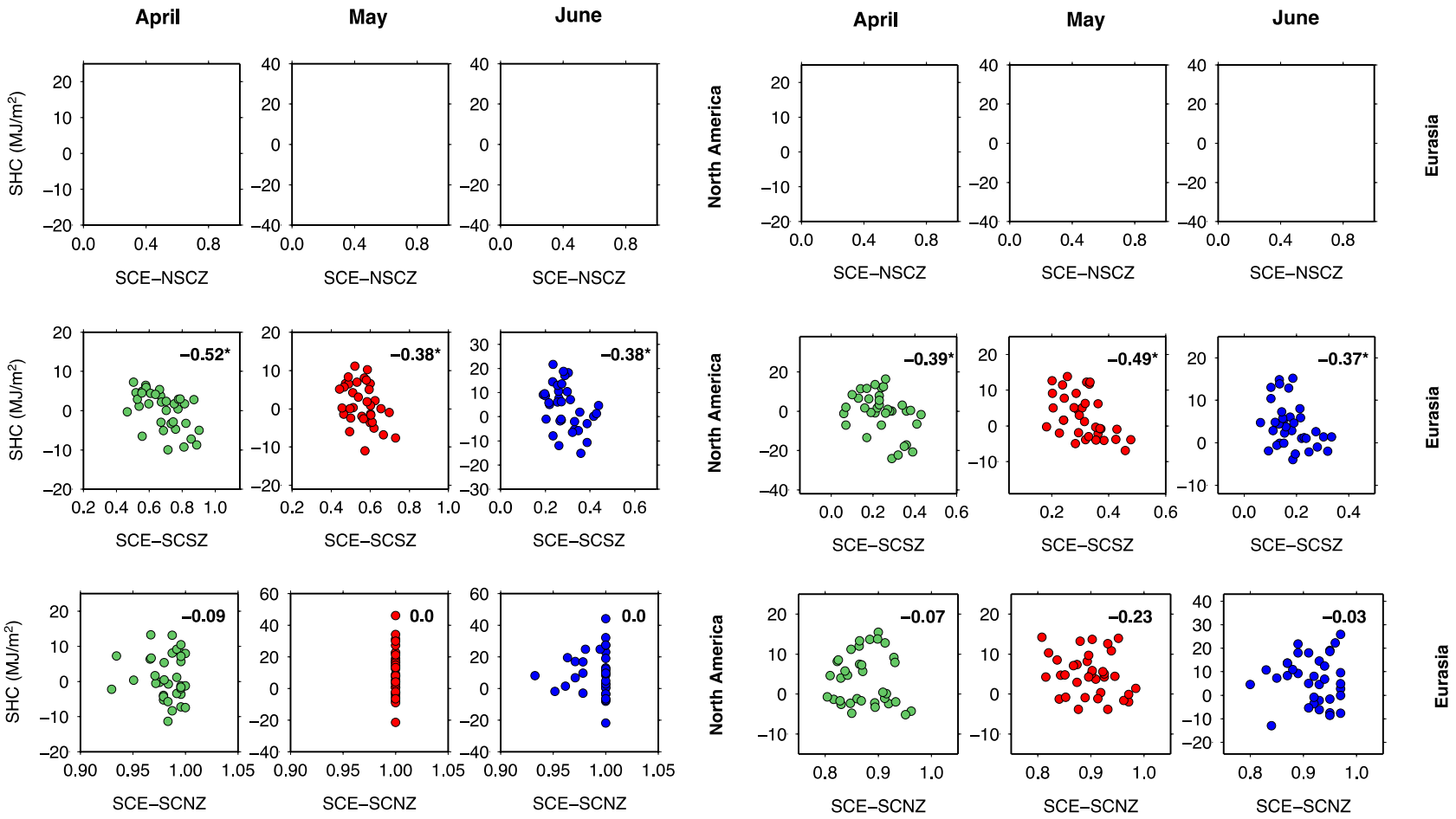

Figure 5. Correlations between observed SCE and simulated SHC in NSCZ, SCSZ, and SCNZ over North America and Eurasia from April through June for the period 1972-2006. The correlation is statistically significant at a level of $p < 0.025$ when its absolute value is greater than 0.34.

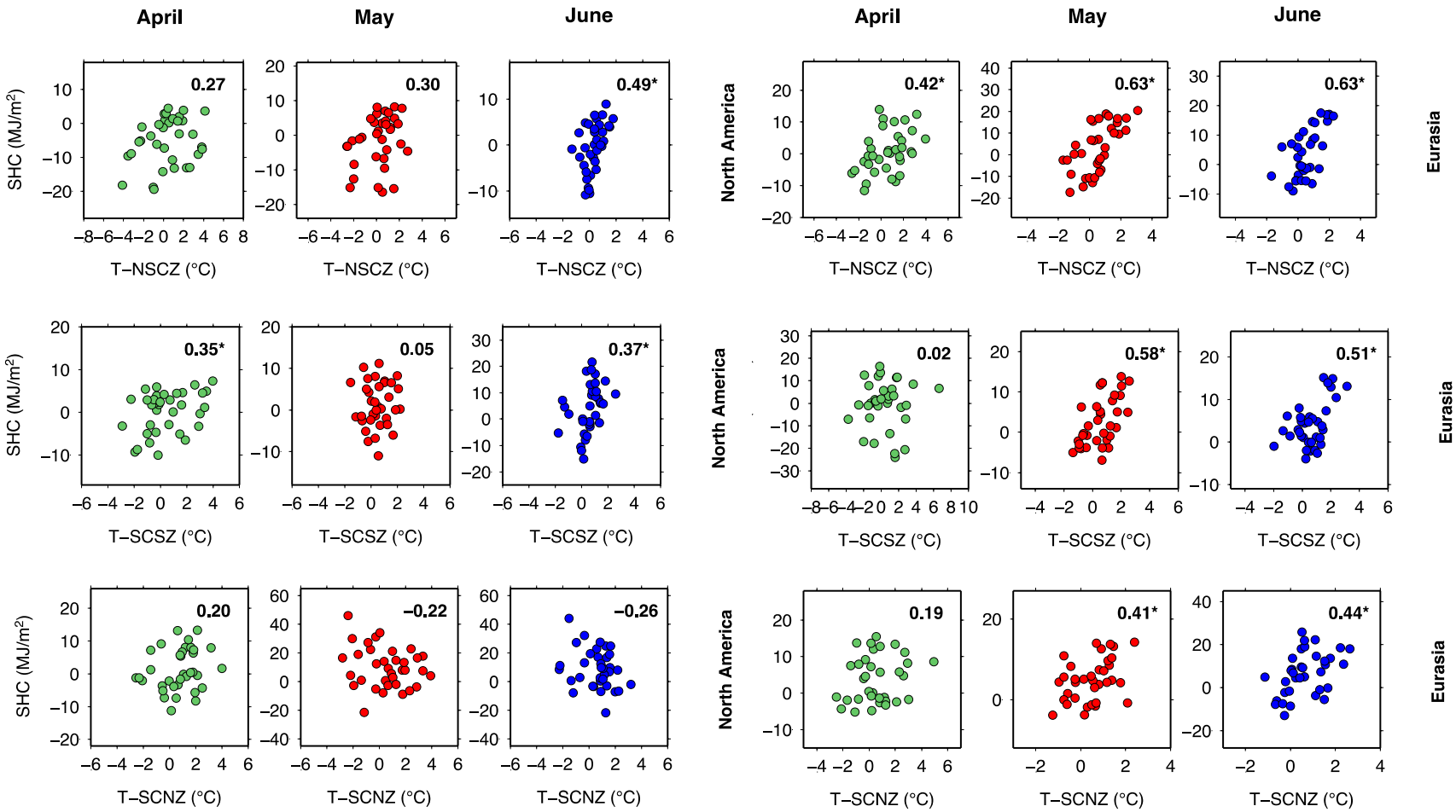

Figure 6. Correlations between observed SAT and simulated SHC in NSCZ, SCSZ and SCNZ over North America and Eurasia from April through June for the period 1972-2006. The correlation is statistically significant at a level of $p < 0.025$ when its absolute value is greater than 0.34.

553

List of Tables

Table 1. Trend analyses for observed snow cover extent (SCE) in the snow covered sensitivity zone (SCSZ) and the snow covered non-sensitivity zone (SCNZ) over North America and Eurasia from April through June for the period 1972-2006. The significance level (*p*-value) was calculated using a two-sided Mann-Kendall trend test. Trend slope (ts) units are $year^{-1}$.

554

Table 2. Trend analyses for CRU monthly surface air temperature (SAT) in the non-snow covered zone (NSCZ), SCSZ, and SCNZ over North America and Eurasia from April through June for the period 1972-2006. The significance level (*p*-value) was calculated using a two-sided Mann-Kendall trend test. Ts units are $°C year^{-1}$.

Table 3. Eighteen soil thermal nodes (STN) and their corresponding depth (m) from the surface. The first STN has a depth of 0 m indicating it is at the surface.

555

556 **Table 4.** Correlation coefficients due to the linear trend and variability for SHC derived from
557 VIC and NOAA-SCE observations in SCSZ and SCNZ over North America and Eurasia from
558 April to June for the period 1972-2006. The significance level (*p*-value) was calculated using
559 a two-tailed Student t-test with 33 degrees of freedom.

Table 5. Correlation coefficients due to the linear trend and variability for SHC derived from VIC and CRU SAT in NSCZ, SCSZ, and SCNZ over North America and Eurasia from April to June for the period 1972-2006. The significance level (*p*-value) was calculated using a two-tailed Student t-test with 33 degrees of freedom.

Table 1. Trend analyses for observed snow cover extent (SCE) in the snow covered sensitivity zone (SCSZ) and the snow covered non-sensitivity zone (SCNZ) over North America and Eurasia from April through June for the period 1972-2006. The significance level (*p*-value) was calculated using a two-sided Mann-Kendall trend test. Trend slope (ts) units are $year^{-1}$.

560

	North America						**Eurasia**					
	April		May		June		April		May		June	
	p <	ts	*p* <	ts	*p* <	ts	*p* <	ts	*p* <	ts	*p* <	ts
SCE-SCSZ	0.025	-0.0052	0.01	-0.0026	0.01	-0.0029	0.025	-0.0042	0.01	-0.0035	0.005	-0.0034
SCE-SCNZ	--	-0.0002	--	-0.0000	--	-0.0000	--	0.0003	--	-0.0010	--	-0.0006

Table 2. Trend analyses for CRU monthly surface air temperature (SAT) in the non-snow covered zone (NSCZ), SCSZ, and SCNZ over North America and Eurasia from April through June for the period 1972-2006. The significance level (*p*-value) was calculated using a two-sided Mann-Kendall trend test. Ts units are $°C year^{-1}$.

	North America						Eurasia					
	April		May		June		April		May		June	
	p <	ts	*p* <	ts	*p* <	ts	*p* <	ts	*p* <	ts	*p* <	ts
SAT-NSCZ	--	0.0345	--	-0.0243	0.005	0.0323	--	0.0531	0.005	0.0663	0.005	0.0412
SAT-SCSZ	--	0.0400	--	0.0243	0.005	0.0415	--	0.0143	0.005	0.0500	0.005	0.0552
SAT-SCNZ	0.005	0.0657	0.005	0.0806	0.01	0.0467	--	0.0044	0.005	0.0435	0.005	0.0471

564

Table 3. Eighteen soil thermal nodes (STN) and their corresponding depth (m) from the surface. The first STN has a depth of 0 m indicating it is at the surface.

Soil Thermal Node	Depth (m)
STN0	0.0
STN1	0.2
STN2	0.4
STN3	0.6
STN4	0.9
STN5	1.3
STN6	1.7
STN7	2.1
STN8	2.7
STN9	3.3
STN10	4.1
STN11	5.1
STN12	6.1
STN13	7.3
STN14	8.8
STN15	10.6
STN16	12.6
STN17	15.0

565

566

Table 4. Correlation coefficients due to the linear trend and variability for SHC derived from VIC and NOAA-SCE observations in SCSZ and SCNZ over North America and Eurasia from April to June for the period 1972-2006. The significance level (*p*-value) was calculated using a two-tailed Student t-test with 33 degrees of freedom.

			April		May		June	
			$p <$	r	$p <$	r	$p <$	r
Correlation (Trend)	**North America**	SCSZ	0.025	-0.9	0.025	-0.7	0.025	-0.8
		SCNZ	0.025	-0.5	--	0.0	--	0.0
	Eurasia	SCSZ	0.025	-0.9	0.025	-1.0	0.025	-0.8
		SCNZ	0.025	0.9	0.025	-0.7	0.025	-0.7
Correlation (Variability)	**North America**	SCSZ	--	-0.2	--	-0.1	--	0.0
		SCNZ	--	0.0	--	0.0	--	0.0
	Eurasia	SCSZ	--	-0.0	--	-0.0	--	0.1
		SCNZ	--	-0.1	--	-0.1	--	0.1

571

Table 5. Correlation coefficients due to the linear trend and variability for SHC derived from VIC and CRU SAT in NSCZ, SCSZ, and SCNZ over North America and Eurasia from April to June for the period 1972-2006. The significance level (*p*-value) was calculated using a two-tailed Student t-test with 33 degrees of freedom.

			April		**May**		**June**	
			p <	*r*	*p* <	*r*	*p* <	*r*
Correlation (Trend)	**North America**	NSCZ	0.025	0.3	0.025	-0.7	0.025	0.7
		SCSZ	0.025	0.9	0.025	0.7	0.025	0.8
		SCNZ	0.025	0.5	--	0.0	--	0.0
	Eurasia	NSCZ	0.025	0.9	0.025	1.0	0.025	1.0
		SCSZ	0.025	0.9	0.025	1.0	0.025	0.8
		SCNZ	0.025	1.0	0.025	0.7	0.025	0.7
Correlation (Variability)	**North America**	NSCZ	--	0.2	0.025	0.4	--	0.37
		SCSZ	--	0.1	--	-0.2	--	-0.1
		SCNZ	--	-0.0	--	-0.2	--	-0.2
	Eurasia	NSCZ	--	0.2	--	0.1	--	0.2
		SCSZ	--	0.0	--	0.2	--	0.1
		SCNZ	--	0.1	--	0.1	--	0.1

572